

1 The formation and evolution of submarine headless channels

2

3 **Ye Chen**<sup>1,2</sup>, Rebecca Williams<sup>2</sup>, Stephen M. Simmons<sup>1</sup>, Matthieu J.B. Cartigny<sup>3</sup>, Maarten S.  
4 Heijnen<sup>4,5</sup>, Daniel R. Parsons<sup>1</sup>, John E. Hughes Clarke<sup>6</sup>, Cooper D. Stacey<sup>7</sup>, Sophie Hage<sup>4,8</sup>,  
5 Peter J. Talling<sup>3</sup>, Ed L. Pope<sup>3</sup>; Maria Azpiroz-Zabala<sup>4,9</sup>, Michael A. Clare<sup>4</sup>, Catharina J.  
6 Heerema<sup>3</sup>; Jamie L. Hizzett<sup>4,5</sup>, James E. Hunt<sup>4</sup>, D. Gwyn Lintern<sup>7</sup>, Esther J. Sumner<sup>5</sup>, Age J.  
7 Vellinga<sup>4,5</sup>, Daniela Vendettuoli<sup>4,5</sup>

8

9 <sup>1</sup>Energy and Environment Institute, University of Hull, Hull, HU6 7RX, UK

10 <sup>2</sup>Department of Geography, Geology and Environment, University of Hull, Hull, HU6 7RX,  
11 UK

12 <sup>3</sup>Departments of Earth Sciences and Geography, University of Durham, Stockton Road,  
13 Durham, DH1 3LE, UK

14 <sup>4</sup>School of Ocean and Earth Sciences, University of Southampton, Southampton SO14 3ZH,  
15 UK

16 <sup>5</sup>Ocean Biogeoscience, National Oceanography Centre, Southampton SO14 3ZH, UK

17 <sup>6</sup>Center for Coastal and Ocean Mapping, University of New Hampshire, Durham, New  
18 Hampshire 03824, USA

19 <sup>7</sup>Natural Resource Canada, Geological Survey of Canada, Sidney, British Columbia V8L  
20 4B2, Canada

21 <sup>8</sup>Department of Geoscience, University of Calgary, Calgary, T2N 1N4 AB, Canada

22 <sup>9</sup>Faculty of Civil Engineering and Geosciences, Delft University of Technology, Delft, The  
23 Netherlands

24

25 **Email: Ye.Chen-2016@hull.ac.uk**

26

27 This is a non-peer reviewed preprint submitted to EarthArXiv. This manuscript has  
28 been submitted to Geology for peer review. Subsequent versions of this manuscript  
29 may have slightly different content. Please feel free to contact any of the authors. We  
30 welcome feedback.

31

32

33

34

35

36

37

38

39

40

41

42

43

44           **The formation and evolution of submarine headless channels**

45   **Ye Chen**<sup>1,2</sup>, Rebecca Williams<sup>2</sup>, Stephen M. Simmons<sup>1</sup>, Matthieu J.B. Cartigny<sup>3</sup>, Maarten S.  
46 Heijnen<sup>4,5</sup>, Daniel R. Parsons<sup>1</sup>, John E. Hughes Clarke<sup>6</sup>, Cooper D. Stacey<sup>7</sup>, Sophie Hage<sup>4,8</sup>, Peter  
47 J. Talling<sup>3</sup>, Ed L. Pope<sup>3</sup>; Maria Azpiroz-Zabala<sup>4,9</sup>, Michael A. Clare<sup>4</sup>, Catharina J. Heerema<sup>3</sup>;  
48 Jamie L. Hizzett<sup>4,5</sup>, James E. Hunt<sup>4</sup>, D. Gwyn Lintern<sup>7</sup>, Esther J. Sumner<sup>5</sup>, Age J. Vellinga<sup>4,5</sup>,  
49 Daniela Vendettuoli<sup>4,5</sup>

50   <sup>1</sup>Energy and Environment Institute, University of Hull, Hull, HU6 7RX, UK

51   <sup>2</sup>Department of Geography, Geology and Environment, University of Hull, Hull, HU6 7RX, UK

52   <sup>3</sup>Departments of Earth Sciences and Geography, University of Durham, Stockton Road,  
53 Durham, DH1 3LE, UK

54   <sup>4</sup>Ocean Biogeoscience, National Oceanography Centre, Southampton SO14 3ZH, UK

55   <sup>5</sup>School of Ocean and Earth Sciences, University of Southampton, Southampton SO14 3ZH, UK

56   <sup>6</sup>Center for Coastal and Ocean Mapping, University of New Hampshire, Durham, New  
57 Hampshire 03824, USA

58   <sup>7</sup>Natural Resource Canada, Geological Survey of Canada, Sidney, British Columbia V8L 4B2,  
59 Canada

60   <sup>8</sup>Department of Geoscience, University of Calgary, Calgary, T2N 1N4 AB, Canada

61   <sup>9</sup>Faculty of Civil Engineering and Geosciences, Delft University of Technology, Delft, The  
62 Netherlands

63

64 **Abstract:** The scale of submarine channels can rival or exceed those formed on land and  
65 they form many of the largest sedimentary deposits on Earth. Turbidity currents that carve  
66 submarine channels pose a major hazard to offshore cables and pipelines, and transport  
67 globally significant amounts of organic carbon. Alongside the primary channels, many systems  
68 also exhibit a range of headless channels, which often abruptly terminate at steep headscarps.  
69 These enigmatic features are widespread in lakes and ocean floors, either as branches off the  
70 main submarine channel thalweg or as isolated secondary channels. Prior research has  
71 proposed that headless channels may be associated with early and incipient stages of channel  
72 development, but their formation and evolution remain poorly understood. Here, we  
73 investigate the morphology, origin and development of headless channels by examining  
74 repeat bathymetric surveys spanning a period from 1986 to 2018, in Bute Inlet, Canada. We  
75 show how channel switching processes, the extension of turbidity currents across distal fans,  
76 along with overbanking turbidity currents, are able to initiate headless channels in submarine  
77 settings. We discuss how the evolution of headless channels plays an important role in  
78 shaping submarine channels, promoting channel extension and modifying the overall  
79 longitudinal profile, as well as impacting the character of sedimentary records in channel-lobe  
80 transition zones.

81

## 82 **INTRODUCTION**

83 Submarine channels act as the primary conduits for the delivery of globally significant  
84 amounts of sediment, pollutant and organic carbon into the deep-sea (e.g., Bouma, 2000;  
85 Paull et al., 2011; Hage et al., 2020; Zhong and Peng, 2021). They extend over distances of  
86 hundreds of kilometres (e.g. Talling et al., 2013) and pose significant hazards to offshore

87 infrastructure (Carter et al., 2014). Although submarine channel inception and subsequent  
88 development have drawn significant attention in the last few decades (Imran et al., 1998;  
89 Covault et al., 2014; De Leeuw et al., 2016), limited work has been undertaken on the  
90 formation and evolution of headless channels. These enigmatic features can branch off the  
91 main channel thalweg or exist as isolated secondary channels, often exhibiting a steep break  
92 in slope at the channel head, which can often take the form of a headscarp. They have been  
93 observed both on lake floors (Girardclos et al., 2012; Turmel et al., 2015; Corella et al., 2016)  
94 and within submarine systems (Paull et al., 2011; Gales et al., 2019).

95 Despite their wide occurrence, the role of headless channel in the generation and evolution  
96 of submarine channel systems is uncertain, especially as headless channels do not connect to  
97 obvious sources for turbidity currents, such as river mouths. Previous research has suggested  
98 that submarine channels themselves are initiated or extended by trains of scours that are  
99 likely formed by the interaction of overriding turbidity currents with seafloor perturbations  
100 (Fildani and Normark, 2004; Covault et al., 2014). Zones where turbidity currents spread  
101 laterally as a result of a transition from confined to unconfined environments are favourable  
102 locations for new channel formation (e.g. Fildani et al., 2006). Channelization across  
103 subaqueous fans by overpassing turbidity currents have been suggested as a mechanism that  
104 can induce avulsion (e.g. Yu et al., 2006) with channel abandonment and channel filling  
105 thereby resulting in the formation of abandoned headless channels (Hamilton et al., 2015).  
106 Additionally, Fildani and Normark (2004) have suggested that initiation of such new flow  
107 pathways is often preceded by discontinuous channel features, consisting of a series of scours  
108 produced by the overspilling turbidity currents (Maier et al., 2011; Fildani et al., 2013; Covault  
109 et al., 2014). These incipient channels can form basinward of the main channel system, with  
110 their connectivity leading to overall downstream channel extension (Fildani et al., 2013;

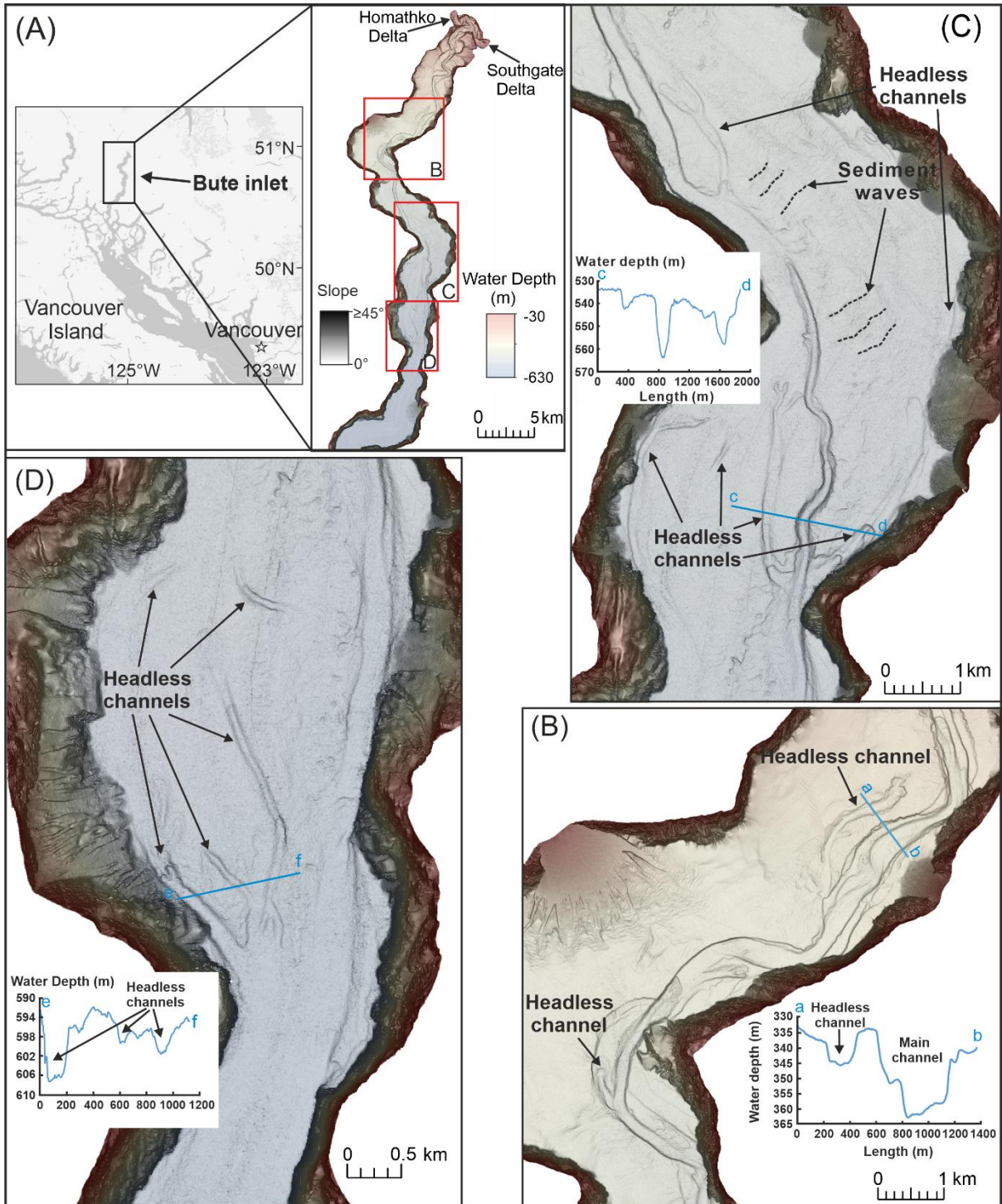
111 Hamilton et al, 2015; Pohl et al., 2019). As such, the formation and evolution of headless  
112 channels is likely to play an important role in channel inception and longer-term downstream  
113 extension of channel systems as well as controlling long-term sedimentary architecture.

114 In this study, we examine the morphodynamics of submarine headless channels using a >30  
115 years (1986-2018) record of bathymetric surveys, extending from source to sink, from the  
116 submarine channel system in Bute Inlet, Canada. Our aims are to understand: (1) the spatial  
117 and temporal distribution and evolution of submarine headless channels; (2) how headless  
118 channels are formed in different settings, such as channel-lobe transition zone (CLTZ), within  
119 distal fan region and within channel overbank areas, and (3) how headless channels affect  
120 downstream channel extension and wider channel system evolution, and the subsequent  
121 deposits that are preserved in the sedimentary record.

122

## 123 **STUDY SITE AND METHODS**

124 Bute Inlet is a fjord located on the SW coastline of British Columbia, Canada (Fig. 1). A sandy  
125 floored submarine channel is incised into Holocene fjord-bottom silts and clays, created by  
126 turbidity currents from the Homathko and Southgate River deltas at the fjord head (Zeng et  
127 al., 1991; Heijnen et al., 2020). The submarine channel extends over 44 km and reaches water  
128 depths of >600 m (Prior et al., 1987; Chen et al., 2021).



129

130 *Figure 1. Submarine channel morphology and locations of headless channels within the fjord. (A)*  
 131 *Location of Bute Inlet in British Columbia, Canada. (B-D) mark locations of headless channels and*  
 132 *sediment waves from the middle to lower reaches of the submarine channel system. The cross-*  
 133 *sectional profiles of headless channels and main channel are shown inset within (B) (C) and (D).*

134

135 An unprecedented dataset comprising a sequence of repeat high-resolution bathymetric  
136 surveys has allowed quantification of the fjord seafloor morphodynamics from 2008 to 2018.  
137 These data were collected using either a Kongsberg-Simard EM1002 or more recently a  
138 Kongsberg EM710 multibeam system, with a vertical resolution of  $\sim 0.5\%$  and horizontal  
139 resolution of  $\sim 3\%$  of water depth (Heijnen et al., 2020). Data were processed using CARIS-  
140 HIPS software, with the employment of POSPac processing suite to improve the positional  
141 accuracy of the vessel using coincident data from fixed regional GPS stations. In addition to  
142 these more recent bathymetric surveys, published results from a previous field survey, which  
143 employed position interpolated sidescan sonar (Prior et al., 1986, 1987), are included in this  
144 study in order to explore the longer-term planform channel changes over an extended 30-  
145 year period. Some caution is needed in terms of the positional accuracy and the detailed  
146 interpretations of the older sidescan survey. However, comparison of identified features and  
147 broader pattern between the 1986 survey and more recent bathymetric surveys shows  
148 significant, larger-scale changes in channel location, as well as downstream channel extension.

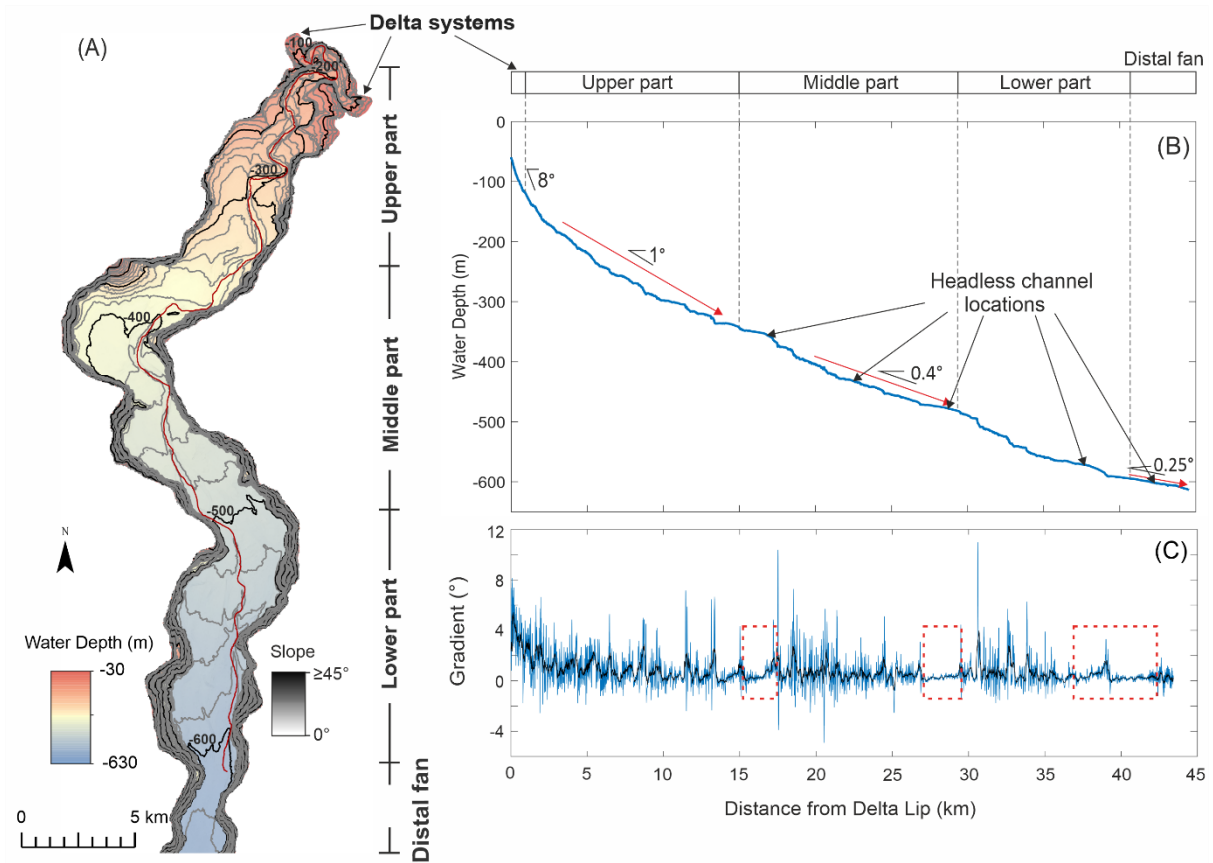
149

## 150 **RESULTS**

151 The overall fjord seafloor profile exhibits a concave-upward section proximal to the deltas  
152 with a reduction in mean gradient through the middle and lower parts of the system (Fig. 2).  
153 The channel system is herein classified into five sections (Fig. 2A): (1) at the fjord-head, two  
154 freshwater delta systems clinofolds with superimposed crescentic bedforms; (2) an upper,  
155 sinuous confined channel (up to 40 m depth) that extends from the deltas to  $\sim 15$  km along  
156 the channel course with a lack of headless channel features throughout the zone; (3) a middle-  
157 part, lower-gradient section that extends from  $\sim 15$  km to  $\sim 29$  km, with a number of headless



158 channels on the main channel flanks; (4) a lower channel part comprising a channel-lobe  
 159 transition zone (CLTZ), extending from ~29 km to 41 km, where headless channels are  
 160 common; and (5) a broad distal depositional fan at the end of the channel.



161  
 162 *Figure 2. (A) Bathymetric map of Bute Inlet showing the broad channel classification system adopted*  
 163 *herein. Red line denotes the channel thalweg from October 2016; (B) Profile along the channel thalweg*  
 164 *and locations of headless channels, demonstrating that channel slope gradient decreases from ~8° at*  
 165 *the delta to below 0.25° at the distal area; (C) Blue line denotes the gradient of channel longitudinal*  
 166 *profile derived from each 1 m pixel. Black line denotes a moving average (10 midpoint) of slope*  
 167 *gradient. The red dashed boxes highlight three low-gradient regions along the profile.*

168  
 169 Headless channels are thus predominantly observed from the middle to lower part of the  
 170 channel system (Fig. 1B, C, D), where slope gradients are generally below 0.5°. The submarine

171 channel becomes less entrenched downstream and is also dominated by large knickpoints  
172 (Heijnen et al., 2020; Chen et al., 2021). Sediment waves are also present in the overbank  
173 areas along the lower part of the channel (Fig. 1C).

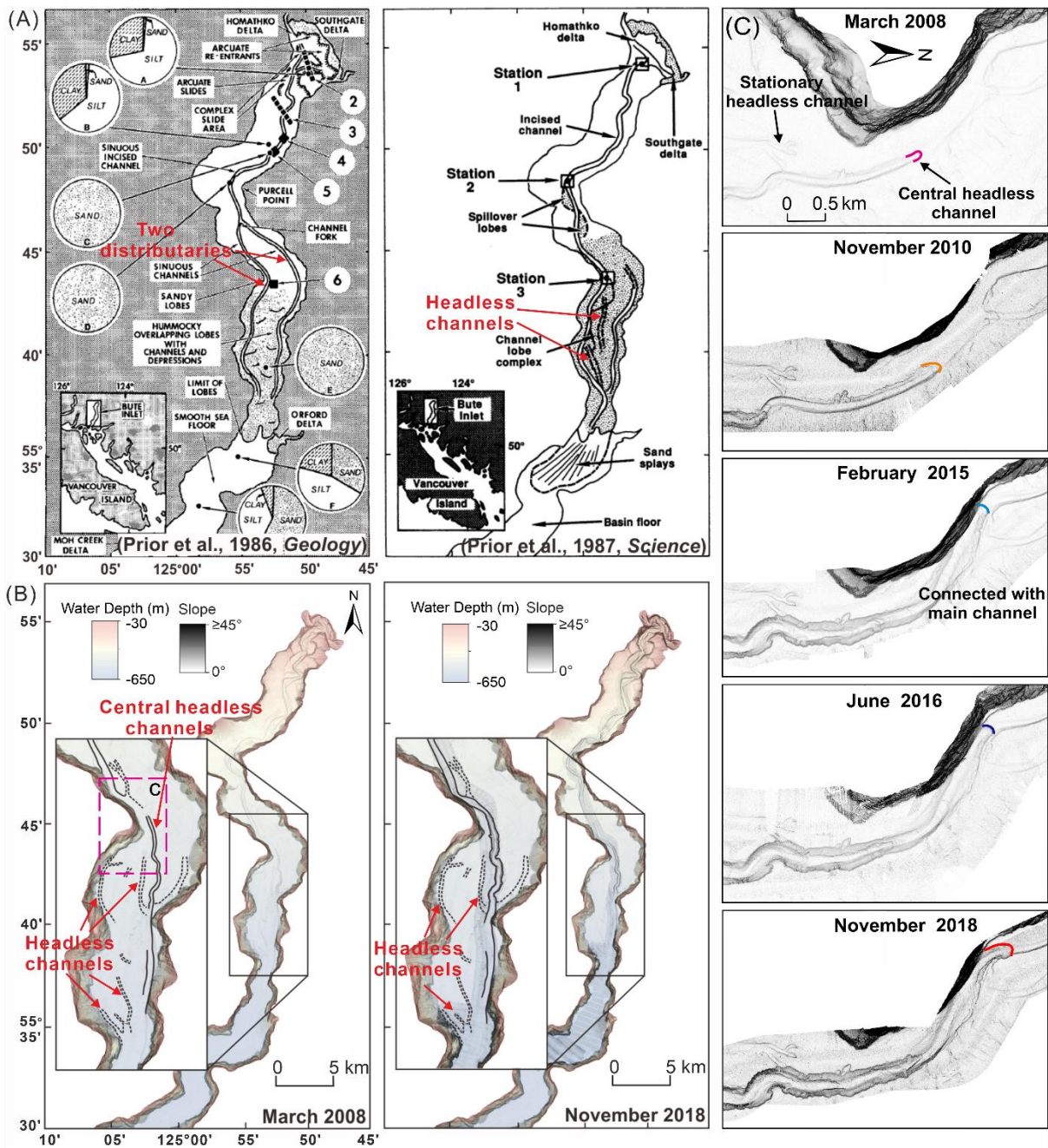
174 Comparison of the field data from 1986 to 2008 reveal clear morphological changes in the  
175 channel location within the lower channel section and across the distal fan (Fig. 3A and Fig.  
176 3B). The 1986 sidescan survey was interpreted to show two main channels along both margins  
177 of the fjord seafloor (Fig. 3A), although there is uncertainty over how they connected in this  
178 lower resolution sidescan data (Prior et al., 1987). The bathymetric data, from 2008-2018,  
179 reveals that a small headless channel was initially formed on the central fjord seafloor but  
180 was disconnected from main channel in the 2008 survey (Fig. 3B, 3C). The evolution of this  
181 headless channel is captured by subsequent surveys showing how the feature gradually  
182 migrated upstream to connect with the main channel, and result in a single extended overall  
183 channel flow pathway (Fig. 3C). This newly-formed channel section deepened and widened  
184 from 2008 to 2018, until it was similar in cross-sectional area to the upper channel in the 2018  
185 survey. The surveys also reveal how distributary channels are abandoned, highlighting how  
186 remnants of both distributaries can be preserved as headless channels on the seafloor (Fig.  
187 3B). The shift of the submarine channel across the CLTZ over this 30-year period resulted from  
188 channel switching processes, with the initiation and upstream propagation of headless  
189 channels and the subsequent connection with primary channel.

190

## 191 **DISCUSSION**

192 Here, comparison between 1986 and 2008 surveys suggests that channel switching processes  
193 through time in the channel-lobe transition zone (CLTZ) promotes the formation of a new flow

194 pathway and abandonment of former channels (Fig. 3A and B). Similar channel evolution  
195 processes have been observed in sublacustrine channels, in which mass transport deposits  
196 were inferred to regularly cause channel avulsions (Turmel et al., 2015; Corella et al., 2016)  
197 and in river systems, where sediment supply has been linked to avulsion frequency (e.g.  
198 Carlson et al., 2019). In Bute Inlet, the relicts of the former channels are preserved as a suite  
199 of headless channels (Fig. 3B) carved into the fjord floor. We reason, therefore, that channel  
200 switching processes likely cause the formation of submarine headless channels across the  
201 CLTZ (Fig. 4A), and that these system dynamics will be captured and ultimately preserved into  
202 the geological record (e.g. Haughton et al., 2002).



203

204 Figure 3. Morphology evolution of CLTZ in Bute Inlet. (A) Published results from 1986 survey. From left  
 205 to right: Prior et al., 1986; Prior et al., 1987; (B) Data in this study. From left to right: March 2008;  
 206 November 2018. (C) Upstream migration of central headless channel from 2008 to 2018.

207

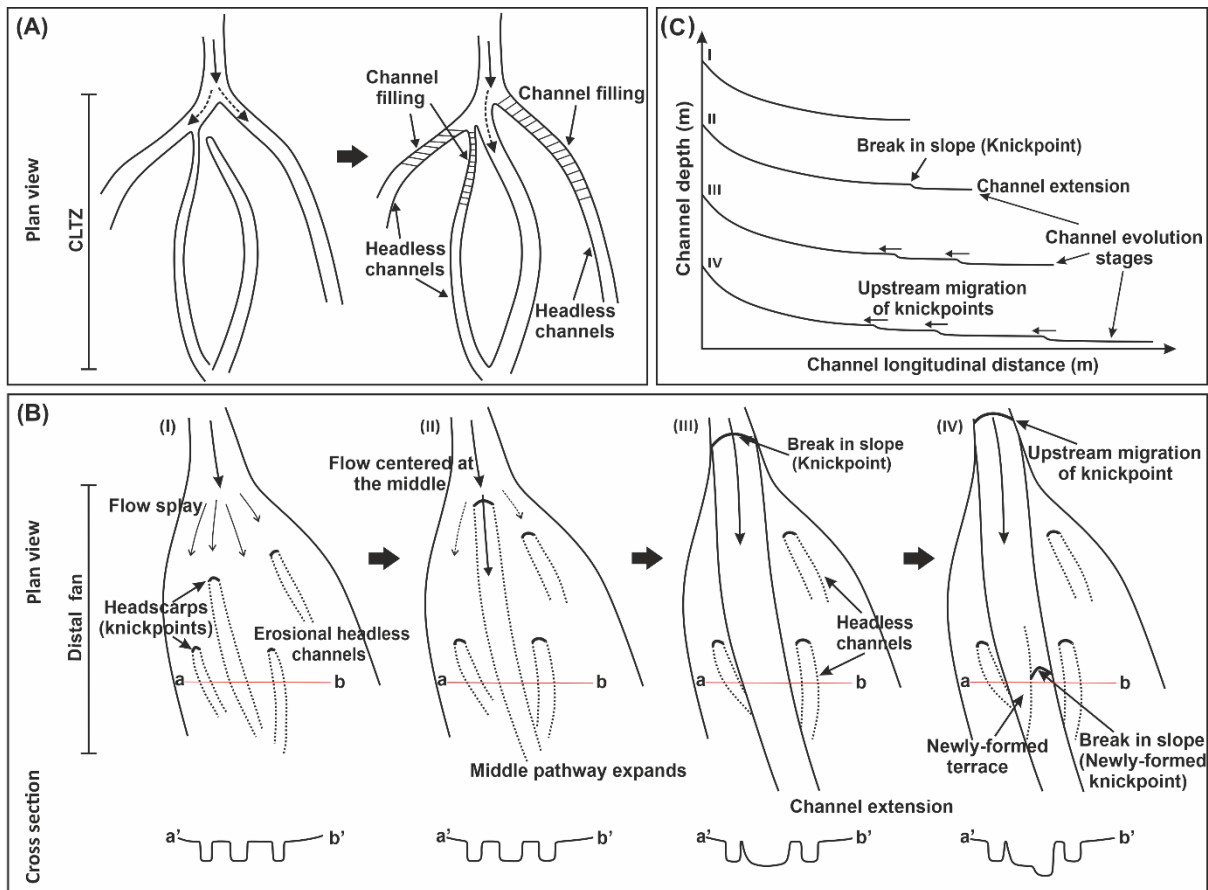
208 The repeat bathymetric data from 2008 to 2018 suggest that the upstream migration of  
 209 erosional headless channels is associated with the loss of turbidity current confinement with

210 the passage through CLTZ and into distal fan region. Laboratory experiments have additionally  
211 shown how loss of lateral confinement can trigger a lowering of the velocity maximum and  
212 an increase in the basal shear stress, which may also cause scours to develop (Pohl et al.,  
213 2019). It is suggested here that the initiation and subsequent propagation of headless  
214 channels seem to result from the migration of these distal erosional scours, which are broadly  
215 similar in form to some megaflutes (Hiscott et al., 2013) or the upstream migration of channel  
216 knickpoints (Heijnen et al., 2020). We reason these scour features may form incipient  
217 headless channels that subsequently migrate upstream, with these small-scale headless  
218 channels eroding up-system during turbidity current flow events. Under such circumstances  
219 headless channels may connect with the primary channel and create an extended conduit,  
220 resulting in channel extension across the distal fan (Fig. 4B, C). Other headless channels will  
221 stop migrating when turbidity currents are newly captured within the new dominant  
222 headless-channel pathway (Fig. 4B). This process results in a series of abandoned headless  
223 channels in the distal fan which will have high preservation potential as the overall channel  
224 system progrades and extends.

225 Headless channels can also form as a result of turbidity currents overflowing channel banks  
226 and re-channelize downslope (e.g., Normark and Piper et al., 1991). Previous analysis of the  
227 submarine channel in Bute Inlet suggests that depositional features (e.g. spill-over lobes),  
228 observed from the middle to lower reaches of the channel and occurred due to turbidity  
229 current flow stripping from the main channel (Fig. 3A, Prior et al., 1986; Zeng et al., 1991).  
230 Elsewhere, linear series of net-erosional scour-shaped depressions/steps are interpreted as  
231 incipient channels offshore California in Monterey East Channel (Fildani et al., 2013), Eel  
232 Canyon (Lamb et al., 2008), and Lucia Chica Channel (Maier et al., 2011). The interactions  
233 between turbidity current overflows and seafloor perturbations in overbank regions could

234 therefore initiate headless channels, or form trains of scours/steps which subsequently merge  
235 to form headless channels (Fildani et al., 2013). The presence of sediment waves in the lower  
236 part of Bute Inlet (Fig. 1C) suggests that turbidity current overflow has occurred and likely  
237 contributed to the formation of headless channels when overspill flows interact with seafloor  
238 perturbations or meet confinement at fjord sides.

239 We propose a general model for the formation and evolution of headless channels and their  
240 interactions with the main channel, which promotes downstream channel extension via the  
241 following steps: (1) a few small headless channels are formed on the distal fan due to  
242 upstream migration of scours, driven by overpassing turbidity current becoming unconfined;  
243 (2) one of the headless channels gradually becomes established and connects with the main  
244 channel, where the initial headscarp of the headless channel may be preserved as a break in  
245 slope (i.e. a knickpoint) that continues to migrate up the main channel; (3) the new channel  
246 section is gradually deepened and widened, and develops terraces (Fig. 4B). Over time, this  
247 channel extension cycle could control both channel longitudinal profile and propagating  
248 knickpoints, and thus dominate long-term submarine channel evolution (Fig. 4C).



249

250 *Figure 4. Conceptual models of (A) channel switching processes; (B) the temporal evolution of headless*  
 251 *channels and interactions with main channel across the distal fan, resulting in channel extension and*  
 252 *the formation of knickpoint; (C) the evolution of channel longitudinal profile with stages showing*  
 253 *channel extension processes and the upstream migration of knickpoints.*

254

255 Headless channels also likely record a distinct seafloor geomorphological signature within the  
 256 geological record, particularly in terms of the different development stages of submarine  
 257 channels (Corella et al., 2016; Gales et al., 2019). Outcrop studies have demonstrated the  
 258 presence of disconnected channels and giant scours, which are interpreted as evidence of a  
 259 temporal shifting of CLTZ (e.g. Hofstra et al., 2015; Brooks et al., 2018). We therefore  
 260 hypothesize that the presence of a suite of headless channels may be used to help infer the  
 261 locations and ancient movements of CLTZ, which in turn could be used to interpret various

262 processes of submarine channel avulsion, channel extension and overall channel system  
263 extension. A range of scales of headless channel have been observed in a variety of submarine  
264 environments globally (e.g. Girardclos et al., 2012; Gales et al., 2019) and these features likely  
265 hold significant potential for improved interpretation of channelization and CLTZ dynamics  
266 across continental margins.

267

## 268 **ACKNOWLEDGEMENTS**

269 Chen was funded by the China Scholarship Council and the University of Hull. We thank the  
270 captains and crews of CCGS *Vector*. We acknowledge UKRI-NERC grants NE/M007138/1,  
271 NE/M017540/1, and ERC Horizon 2020 Grant Agreement 725955 to D.R.P. M.A.C. was  
272 supported by the U.K. National Capability NERC CLASS program NE/R015953/1,  
273 NE/P009190/1 and NE/P005780/1.

274

## 275 **References**

276 Bouma, A.H., 2000, Coarse-grained and fine-grained turbidite systems as end member models:  
277 applicability and dangers: *Marine and Petroleum Geology*, v. 17, p. 137-143,  
278 [https://doi.org/10.1016/S0264-8172\(99\)00020-3](https://doi.org/10.1016/S0264-8172(99)00020-3).

279 Brooks, H.L., Hodgson, D.M., Brunt, R.L., Peakall, J., Hofstra, M. and Flint, S.S., 2018, Deep-water  
280 channel-lobe transition zone dynamics: processes and depositional architecture, an example  
281 from the Karoo Basin, South Africa: *GSA Bulletin*, v. 130, p. 1723-1746,  
282 <https://doi.org/10.1130/B31714.1>

283 Carlson, B.N., Nittrouer, J.A., Moodie, A.J., Kineke, G.C., Kumpf, L.L., Ma, H., Parsons, D.R. and Wang,



284 H., 2020, Infilling abandoned deltaic distributary channel through landward sediment transport:  
285 *JGR Earth surface*, v. 125, e2019JF005254, <https://doi.org/10.1029/2019JF005254>.

286 Carter, L., Gavey, R., Talling, P.J. and Liu, J.T., 2014, Insights into submarine geohazards from breaks  
287 in subsea telecommunication cables. *Oceanography*, 27, 58-67.  
288 <https://doi.org/10.5670/oceanog.2014.40>.

289 Chen, Y., Parsons, D.R., Simmons, S.M., Williams R., Cartigny, M.J.B., Hughes Clarke, J.E., Stacey, C.D.,  
290 Hage, S., Talling, P.J., Azpiroz-Zabala, M., Clare, M.A., Hizzett, J.L., Heijnen, M.S., Hunt, J.E.,  
291 Lintern, D.G., Sumner, E.J., Vellinga, A.J. and Vendettuoli, D. S., 2021, Knickpoints and crescentic  
292 bedform interactions in submarine channels: *Sedimentology*, <https://doi.org/10.1111/sed.12886>.

293 Corella, J.P., Loizeau, J.L., Kremer, K., Hilbe M., Gerard, J., Dantec, N.L., Stark, N., Gonzalez-Quijano,  
294 M., and Girardclos, S., 2016, The role of mass-transport deposits and turbidites in shaping  
295 modern lacustrine deepwater channels: *Marine and Petroleum Geology*, v. 77, p. 515-525,  
296 <https://doi.org/10.1016/j.marpetgeo.2016.07.004>.

297 Covault, J.A., Kostic, S., Paull, C.K., Ryan, H.F., and Fildani, A., 2014, Submarine channel initiation,  
298 filling and maintenance from sea-floor geomorphology and morphodynamic modelling of cyclic  
299 steps: *Sedimentology*, v. 61, p. 1031-1054, <https://doi.org/10.1111/sed.12084>.

300 De Leeuw, J., Eggenhuisen, J. T. and Cartigny, M. J. B., 2016, Morphodynamics of submarine channel  
301 inception revealed by new experimental approach: *Nature Communication*, v. 7, p. 10886,  
302 <https://doi.org/10.1038/ncomms10886>.

303 Fildani, A., and Normark, W.R., 2004, Late Quaternary evolution of channel and lobe complexes of  
304 Monterey Fan: *Marine Geology*, v. 206, p. 199-223,  
305 <https://doi.org/10.1016/j.margeo.2004.03.001>.

306 Fildani, A., Normark, W.R., Kostic, S., and Parker, G., 2006, Channel formation by flow stripping: large-  
307 scale scour features along the Monterey East Channel and their relation to sediment

308 waves: *Sedimentology*, v. 53, p. 1265-1287, <https://doi.org/10.1111/j.1365-3091.2006.00812.x>.

309 Fildani, A., Hubbard, S.M., Covault, J.A., Maier, K.L., Romans, B.W., Traer, M., and Rowland, J.C., 2013,  
310 Erosion at inception of deep-sea channels: *Marine and Petroleum Geology*, v. 41, p. 48-61,  
311 <https://doi.org/10.1016/j.marpetgeo.2012.03.006>.

312 Gales, J.A., Talling, P.J., Cartigny, M.J.B., Clarke, J.H., Lintern, G., Stacey, C., and Clare, M.A., 2019, What  
313 controls submarine channel development and the morphology of deltas entering deep-water  
314 fjords? *Earth Surface Processes and Landforms*, v. 44, p. 535-551,  
315 <https://doi.org/10.1002/esp.4515>.

316 Girardclos, S., Hilbe, M., Corella, J.P., Loizeau, J.L., Kremer, K., Delsontro, T., Arantegui, A., Moscardiello,  
317 A., Arlaud, F., Akhtman, Y., Anselmetti, F.S., and Lemmin, U., 2012, Searching the Rhone delta  
318 channel in Lake Geneva since François alphonse forel. *Archive Des Science*, v. 65, p. 103-118.

319 Hage, S., Galy, V.V., Cartigny, M.J.B., Acikalin, S., Clare, M.A., Gröcke, D.R., Hilton, R.G., Hunt, J.E.,  
320 Lintern, D.G., McGhee, C.A., Parsons, D.R., Stacey, C.D., Sumner, E.J. and Talling, P.J., 2020,  
321 Efficient preservation of young terrestrial organic carbon in sandy turbidity-current deposits:  
322 *Geology*, v. 48, p. 882-887, <https://doi.org/10.1130/G47320.1>.

323 Hamilton, P.B., Strom, K.B., and Hoyal, D.C.J.D., 2015, Hydraulic and sediment transport properties of  
324 autogenic avulsion cycles on submarine fans with supercritical distributaries: *Journal of*  
325 *Geophysical Research Earth Surface*, v. 120, p. 1369-1389,  
326 <https://doi.org/10.1002/2014JF003414>.

327 Haughton, P.D.W., 2002, Evolving turbidite systems on a deforming basin floor, Tabernas, SE Spain:  
328 *Sedimentology*, v. 47, p. 497-518, <https://doi.org/10.1046/j.1365-3091.2000.00293.x>

329 Heijnen, M.S., Clare, M.A., Cartigny, M.J.B., Talling, P.J., Hage, S., Lintern, G., Stacey, C., Parsons, D.R.,  
330 Simmons, S.M., Chen, Y., Sumner, E.J., Dix, J.K., and Hughes Clarke, J.E., 2020, Rapidly-migrating

331 and internally-generated knickpoints can control submarine channel evolution: *Nature*  
332 *Communication*, v. 11, 3129, <https://doi.org/10.1038/s41467-020-16861-x>.

333 Hiscott, R.N., Aksu, A.E., Flood, R.D., Kostylev, V., and Yasar, D., 2013, Widespread overspill from a  
334 saline density-current channel and its interaction with topography on the south-west Black Sea  
335 shelf: *Sedimentology*, v. 60, p. 1639-1667, <https://doi.org/10.1111/sed.12071>.

336 Hofstra, M., Hodgson, D.M., Peakall, J. and Flint, S.S., 2015, Giant scour-fills in ancient channel-lobe  
337 transition zones: formative processes and depositional architecture: *Sedimentary geology*, v. 329,  
338 p. 98-114, <https://doi.org/10.1016/j.sedgeo.2015.09.004>.

339 Hughes Clarke, J. E., 2016, First wide-angle view of channelized turbidity currents links migrating cyclic  
340 steps to flow characteristics. *Nat. Commun.*, 7, 11896, <https://doi.org/10.1038/ncomms11896>.

341 Imran, J., Parker, G. and Katopodes, N.A., 1998, numerical model of channel inception on submarine  
342 fans: *J. Geophys. Res. Ocean*, v. 103, p. 1219-1238, <https://doi.org/10.1029/97JC01721>.

343 Kostic, S., 2011, Modeling of submarine cyclic steps: controls on their formation, migration, and  
344 architecture: *Geosphere*, v. 7, p. 294-304, <https://doi.org/10.1130/GES00601.1>.

345 Lamb, M.P., Parsons, J.D., Mullenbach, B.L., Finlayson, D.P., Orange, D.L., and Nittrouer, C.A., 2008,  
346 Evidence for superelevation, channel incision and formation of cyclic steps by turbidity currents  
347 in Eel Canyon, California: *Geological Society of America Bulletin*, v. 120, p. 463-475,  
348 <https://doi.org/10.1130/B26184.1>.

349 Maier, K.L., Fildani, A., Paull, C.K., Graham, S.A., McHargue, T., Caress, D., and McGann, M., 2011, The  
350 elusive character of discontinuous deep-water channels: new insights from Lucia Chica channel  
351 system, offshore California: *Geology*, v. 39, p. 327-330, <https://doi.org/10.1130/G31589.1>.

352 Normark, W.R., and Piper D.J.W., 1991, Initiation processes and flow evolution of turbidity currents:  
353 implications for the depositional record: AAPG Special Publications of SEPM.

354 Paull, C.K., Caress, D.W., Iij, W.U., Lundsten, E., and Meiner-johnson, M., 2011, High-resolution  
355 bathymetry of the axial channels within Monterey and Soquel submarine canyons, offshore  
356 central California: *Geosphere*, v. 5, p. 1077-1101, <https://doi.org/10.1130/GES00636.1>.

357 Peakall, J. and Sumner, E.J. (2015) Submarine channel flow processes and deposits: A process-product  
358 perspective. *Geomorphology*, 244, 95-120. <https://doi.org/10.1016/j.geomorph.2015.03.005>.

359 Pohl, F., Eggenhuisen, J.T., Tilston, M., and Cartigny, M.J.B., 2019, New flow relaxation mechanism  
360 explains scour fields at the end of submarine channels: *Nature Communication*, v. 10, 4425,  
361 <https://doi.org/10.1038/s41467-019-12389-x>.

362 Prior, D.B., Bornhold, B.D., and Johns, M.W., 1986, Active sand transport along a fjord-bottom channel,  
363 Bute inlet, British Columbia: *Geology*, v. 14, p. 581-584, [https://doi.org/10.1130/0091-7613\(1986\)14<581:ASTAAF>2.0.CO;2](https://doi.org/10.1130/0091-7613(1986)14<581:ASTAAF>2.0.CO;2).

365 Prior, D.B., Bornhold, B.D., Wiseman, W.J., and Lowe, D.R., 1987, Turbidity Current Activity in a British  
366 Columbia Fjord: *Science*, v. 237, p. 1330-1333, DOI: 10.1126/science.237.4820.1330.

367 Talling, P.J., Paull, C.K. and Piper, D.J.W. (2013) How are subaqueous sediment density flows triggered,  
368 what is their internal structure and how does it evolve? Direct observations from monitoring of  
369 active flows. *Earth. Sci. Rev.*, v. 125, p. 244-287. <https://doi.org/10.1016/j.earscirev.2013.07.005>.

370 Turmel, D., Locat, J., and Parker, G., 2015, Morphological evolution of a well-constrained, subaerial  
371 subaqueous source to sink system: Wabush Lake: *Sedimentology*, v. 62, p. 1636-1664,  
372 <https://doi.org/10.1111/sed.12197>.

373 Yu, B., Cantelli, A., Marr, J., Pirmez, C., O'Byrne, C., and Parker, G., 2006, Experiments on self-  
374 channelized subaqueous fans emplaced by turbidity currents and dilute mudflows: *Journal of*  
375 *Sedimentary Research*, v. 76, p. 889-902, <https://doi.org/10.2110/jsr.2006.069>.

376 Zeng, J.J., Lowe, D.R., Prior, D.B., Wiseman, W.J., and Bornhold, B.D., 1991, Flow properties of turbidity  
377 currents in Bute inlet, British Columbia: *Sedimentology*, v. 38, p. 975-996,  
378 <https://doi.org/10.1111/j.1365-3091.1991.tb00367.x>.

379 Zhong, G.F., Peng X.T., 2021. Transport and accumulation of plastic litter in submarine canyons—The  
380 role of gravity flows: *Geology*, doi: <https://doi.org/10.1130/G48536.1>

381

382

383

384

385 *Figure 1. Submarine channel morphology and locations of headless channels within the fjord. (A)*  
386 *Location of Bute Inlet in British Columbia, Canada. (B-D) mark locations of headless channels and*  
387 *sediment waves from the middle to lower reaches of the submarine channel system. The cross-*  
388 *sectional profiles of headless channels and main channel are shown inset within (B) (C) and (D).*

389

390 *Figure 2. (A) Bathymetric map of Bute Inlet showing the broad channel classification system adopted*  
391 *herein. Red line denotes the channel thalweg from October 2016; (B) Profile along the channel thalweg*  
392 *and locations of headless channels, demonstrating that channel slope gradient decreases from  $\sim 8^\circ$  at*  
393 *the delta to below  $0.25^\circ$  at the distal area; (C) Blue line denotes the gradient of channel longitudinal*  
394 *profile derived from each 1 m pixel. Black line denotes a moving average (10 midpoint) of slope*  
395 *gradient. The red dashed boxes highlight three low-gradient regions along the profile.*

396

397 *Figure 3. Morphology evolution of CLTZ in Bute Inlet. (A) Published results from 1986 survey. From left*  
398 *to right: Prior et al., 1986; Prior et al., 1987; (B) Data in this study. From left to right: March 2008;*  
399 *November 2018. (C) Upstream migration of central headless channel from 2008 to 2018.*

400

401 *Figure 4. Conceptual models of (A) channel switching processes; (B) the temporal evolution of headless*  
402 *channels and interactions with main channel across the distal fan, resulting in channel extension and*  
403 *the formation of knickpoint; (C) the evolution of channel longitudinal profile with stages showing*  
404 *channel extension processes and the upstream migration of knickpoints.*

405